Online Supplement for "Clay Mineral Variations in Holocene Terrestrial Sediments from the Indus Basin"

Age chronology by AMS radiocarbon and Optically Stimulated Luminescence (OSL) dating

The primary material (Mollusc shells and wood and plant remains) collected for AMS radiocarbon dating were analyzed at the National Ocean Sciences Accelerator Mass Spectrometry facility (NOSAMS) as the Woods Hole Oceanographic Institute, USA. The methodology for AMS radiocarbon dating is presented on the NOSAMS site http://nosams.whoi.edu and discussed in McNichol et al. (1995)

Fluvial and flood plain sand and silt size fraction (90–125 µm) used for OSL dating was prepared under subdued red light conditions at Aberystwyth Luminescence Research Laboratory. The samples were treated with hydrochloric acid and hydrogen peroxide to remove carbonates and organic matter, and afterwards separated with heavy-density liquid ($2.62< \rho <2.70$ $g.cm^3$) to obtained the desired fraction of quartz grains. The obtained quartz grains were etched with hydrofluoric acid to remove the alpha-irradiated outer surface and non-quartz minerals, and after all these processes were ready for OSL analysis.

Sample locations are pointed out on the map of the study area (Fig. 1) in the manuscript and the radiocarbon and OSL ages are graphically shown on the sedimentary logs (Fig. S1). All radiocarbon dates have been converted to calendar ages (2 sigma) using Calib 5.0.1 software (Stuiver et al., 1998) for the shells samples and for wood and plant remains terrestrial IntCal04 calibration of Reimer et al. (2004) were used. For OSL age calibration the Rodnight et al. (2006) method was adopted to choose the appropriate age model.

X-ray diffraction method for clay mineral quantification

X-ray diffraction (XRD) is a reliable and commonly used method for the determination and quantification of clay mineral assemblages. In this study the semi-quantitative method of Moore and Reynolds (1989) is used to estimate the clay assemblage, which is based on peak-intensity factors determined from calculated XRD patterns. Hillier (2003) described the method used in the present study in detail, including its validation and an assessment of analytical uncertainty based on its application to prepared mixtures of pure clay minerals. For clay minerals present in amounts >10 wt %, uncertainty is estimated as better than ±5 wt % at the 95% confidence level. Uncertainty of peak area measurement based on repeated measurements is typically <5%, with the smallest peaks having the highest uncertainties. In addition to calculating the relative percentages of clay minerals in the samples, we also determine various ratios based on measurements of peak areas in the XRD patterns. These ratios are used to reconstruct changes in relative abundance and are directly proportional to ratios calculated from the exact values for individual mineral percentages. Data are presented as both relative percentages and as ratios to best illustrate factors that control trends.

References cited

Alizai, A., Clift, P.D., Giosan, L., et al., 2011. Pb Isotopic Variability in the Modern and Holocene Indus River System measured by Ion Microprobe in detrital K-feldspar grains. Geochimica et Cosmochimica Acta 75, 4771-4795, doi:10.1016/j.gca.2011.05.039.

Clift, P., Giosan, L., Blusztajn, J., et al., 2008. Holocene erosion of the Lesser Himalaya triggered by intensified summer monsoon. Geology 36(1), 79-82, doi: 10.1130/G24315A.1.

Clift, P.D., Carter, A., Giosan, L., et al., in press. U-Pb zircon dating evidence for a Pleistocene Sarasvati River and Capture of the Yamuna River. Geology.

Hillier, S., 2003. Quantitative analysis of clay and other minerals in sandstones by X-ray powder diffraction (XRPD), *in* Worden, R.H., and Morad, S., eds., Clay mineral cements in sandstones: Special Publication, International Association of Sedimentologists.

McNichol, A.P., Gagnon, A.R., Osborne, E.A., Hutton, D.L., VonReden, K.F, Schneider., R.J., 1995. Improvements in procedural blanks at NOSAMS: Reflections of improvements in sample preparation and accelerator operation. Radiocarbon, 37(2), 683–691.

Moore, D., Reynolds, R., 1989. X-ray Diffraction and the Identification and Analysis of Clay Minerals. Oxford, Oxford University Press, 332 p.

Stuiver, M., Reimer, P.J., Bard, E. et al., 1998. INTCAL98 Radiocarbon age calibration. Radiocarbon. 40, 1041–1083.

Reimer, A., Protheroe, R., Donea, A., 2004. M87-a misaligned synchrotron-proton blazar? New Astronomy Reviews 48, 411–413.

Rodnight, H., Duller, G.A.T., Wintle, A.G., Tooth, S., 2006. Assessing the reproducibility and accuracy of optical dating of fluvial deposits. Quaternary Geochronology 1, 109–120.

FIGURE CAPTIONS

Figure S1. Lithological columns for the four core and two trench (in box) sites. Black arrows show available age control presented in this paper. Ages derived from OSL are labelled as such. Ages at Keti Bandar are from Clift et al. (2008), while those at Tilwalla are from Clift et al. (in press). The ages from Marot, Nara and Fort Abbas are from Alizai et al. (2011).

Figure S2. Schematic illustration of sedimentation rate at the Keti Bandar drill site. The age control is obtained from radiocarbon ages (Clift et al., 2008). The average sedimentation rate (cm/yr) is calculated for 13,000 yr. Solid vertical lines are radiocarbon ages and broken lines are 1σ error bars.

Figure S3. Glycolated XRD pattern from contrasting clay mineral assemblages in Tilwalla Core. (A) is from a fine-grained sediment that is relatively poor in smectite (Sm), with evidence of mixed-layering with illite (I/S). Discrete illite (I) is more abundant and of lower crystallinity (wider peaks) and kaolinite (K) is relatively more abundant than chlorite (Ch). In contrast (B) the smectite-rich sample from a sand lense shows no evidence for mixed-layering, i.e. it is end-member smectite, illite is less abundant and more crystalline (sharper peaks) and chlorite is relatively more abundant than kaolinite. The differences shown by these samples are consistent across the Indus flood plain. The patterns are offset vertically for clarity.

Figure S4. Down-core variation in clay minerals at Fort Abbas showing variations in the relative abundance of kaolinite, smectite, illite and chlorite percentages along with chlorite/illite ratio and the crystallinity index for illite. (B) Variations in climate sensitive proxy ratios: s smectite/(illite+chlorite), kaolinite/(illite+chlorite), kaolinite/illite, kaolinite/smectite, kaolinite/chlorite and smectite/illite.

Figure S5. Down-core variation in clay minerals at Fort Derawar showing (A) Variations in the relative abundance of kaolinite, smectite, illite and chlorite percentages, along with chlorite/illite ratio and the crystallinity index for illite. (B) Variations in supposedly climate sensitive proxy ratios: smectite/(illite+chlorite); kaolinite/(illite+chlorite); kaolinite/illite; kaolinite/smectite and smectite/illite.

Table S1. Clay mineral weight percentages from the Punjab and Nara regions analyzed in this study.

Table S2. Clay mineral weight percentages from Keti Bandar located at the Arabian Sea coast, close to the Indus River mouth.

Supplemental Material page-5
Click here to download high resolution image

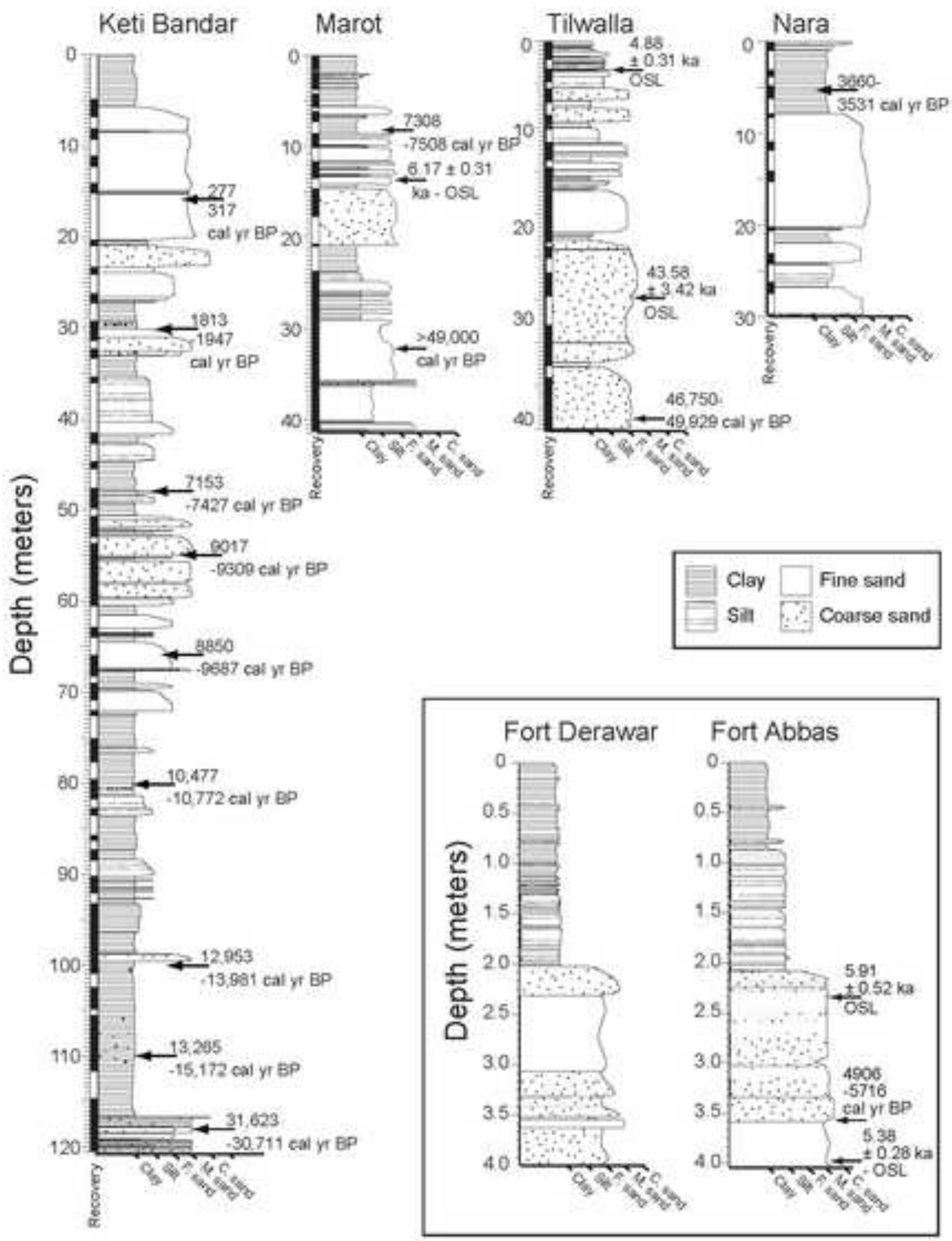

Figure S1
Alizai et al.

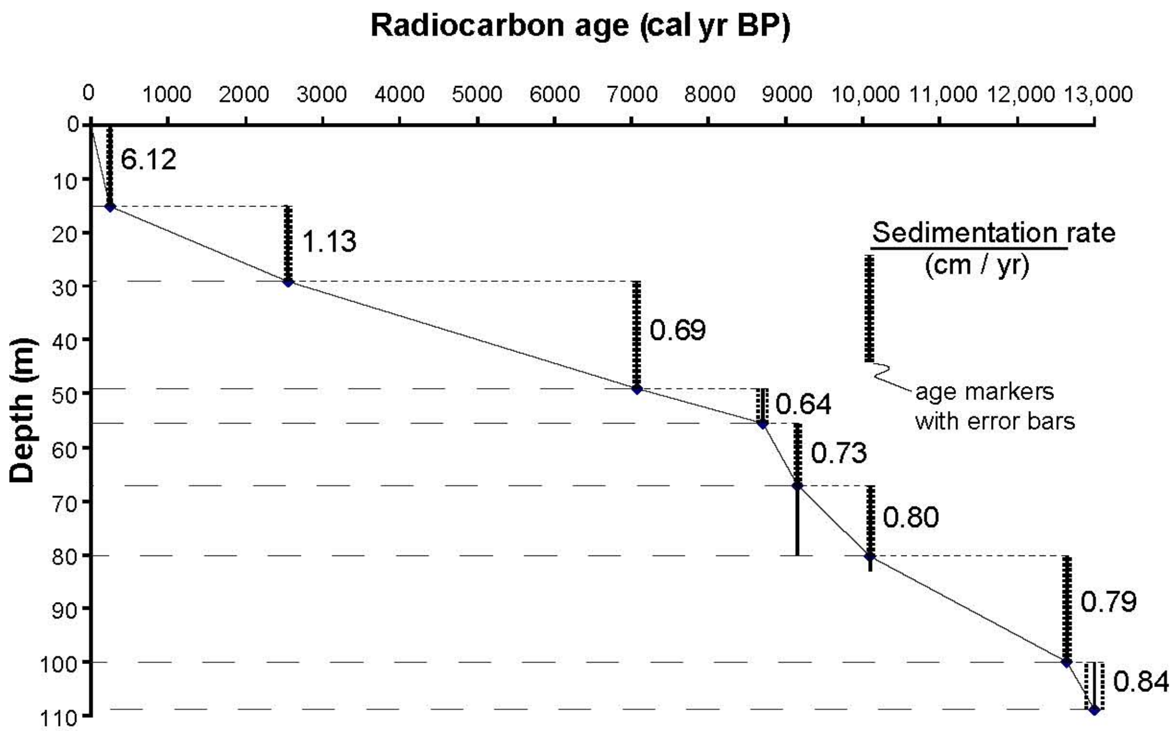

Figure S2
Alizai et al.

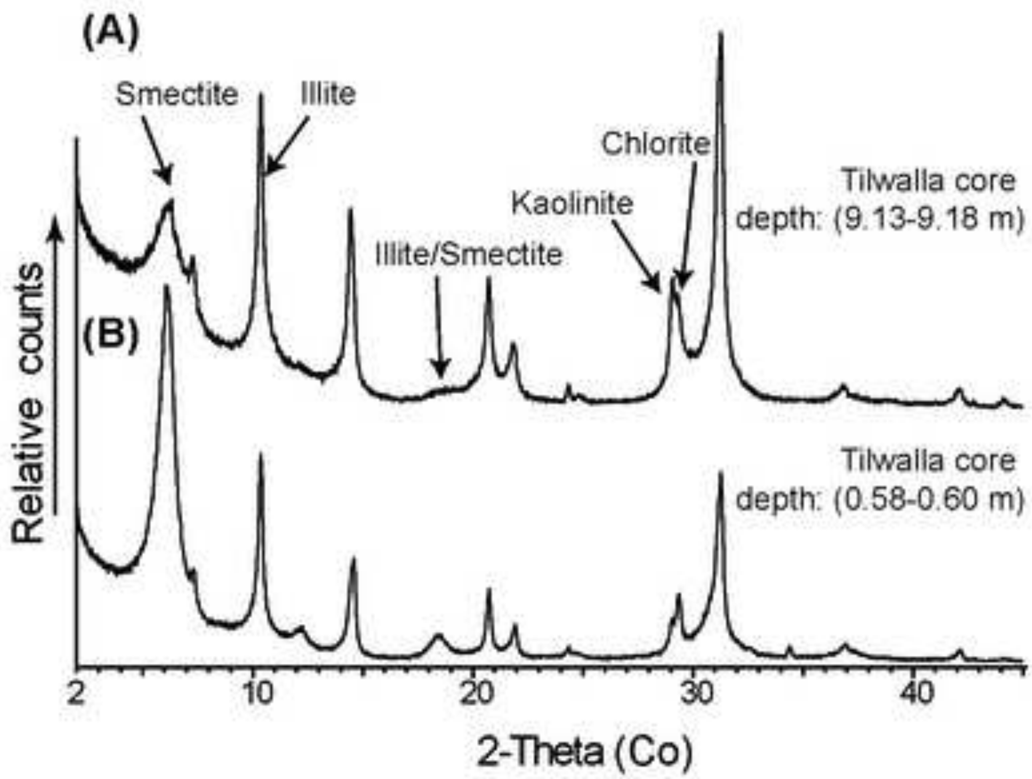

Figure S3
Alizai et al.

Supplemental Material page-8

Click here to download high resolution image

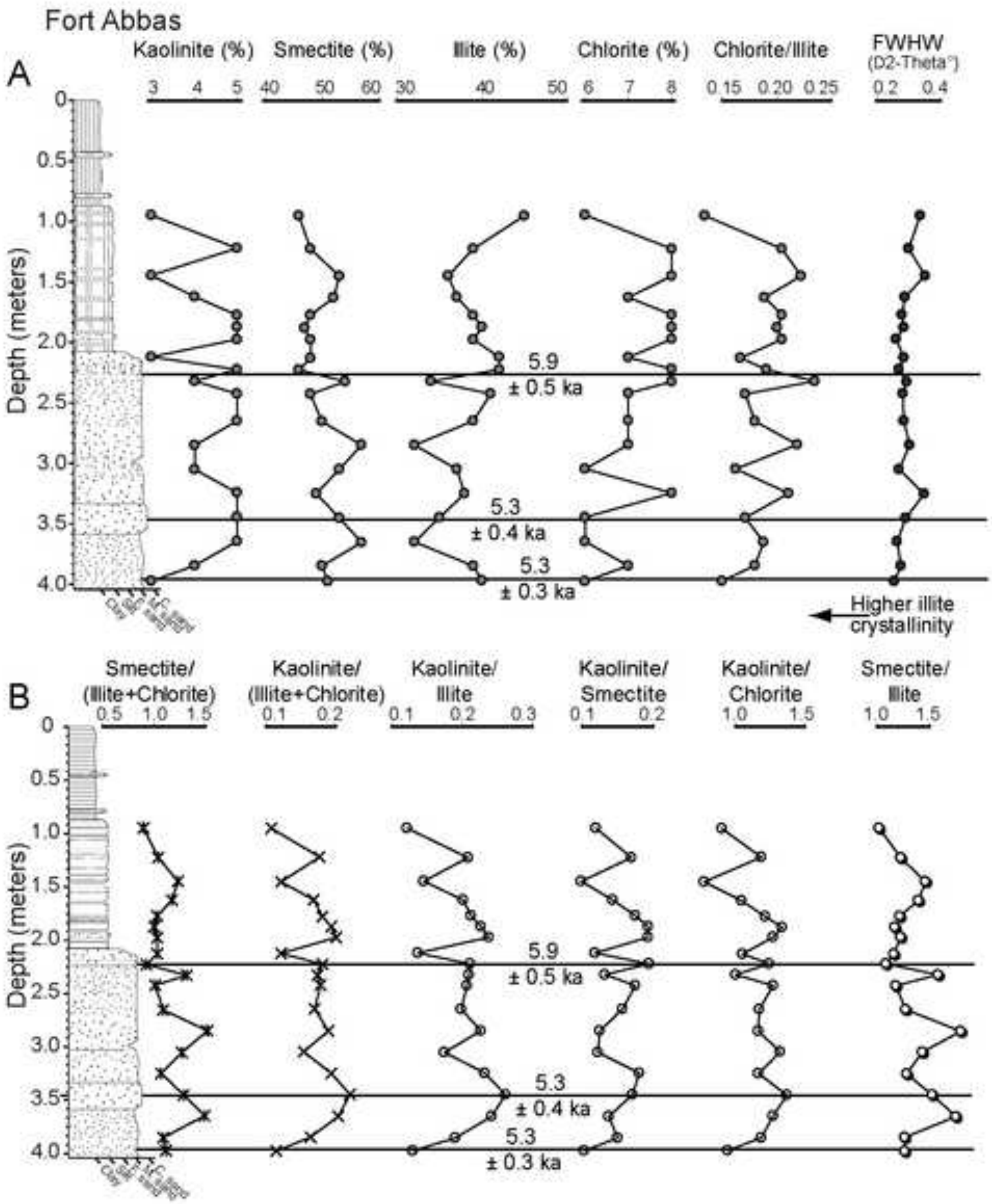

Figure S4
Alizai et al.

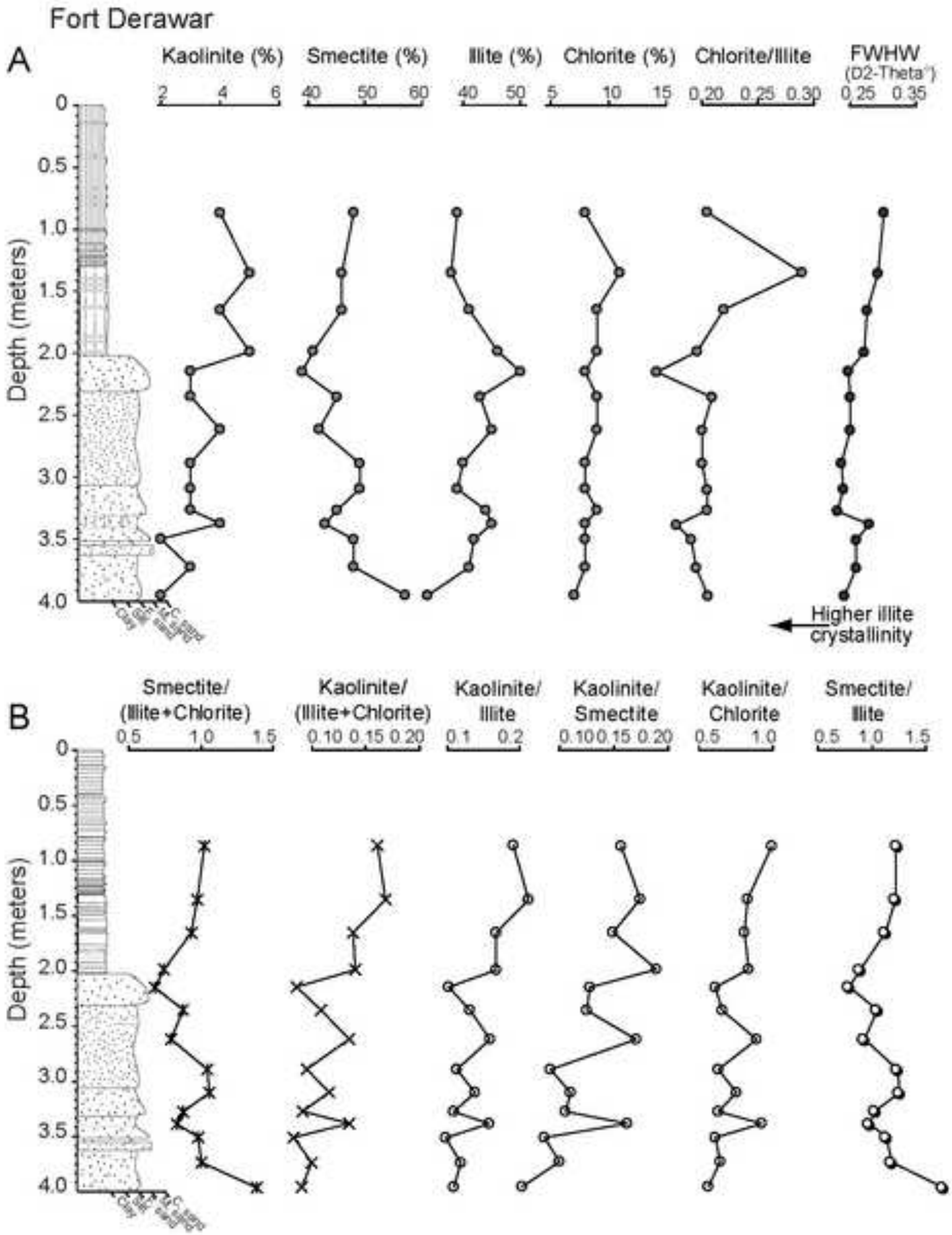

Figure S5
Alizai et al.

Table S1.

Sr. No.	Sample No.	Depth (m)		Kaolinite relative (%)	Chlorite relative (%)	illite relative (%)	Smectite relative (%)	FWHM 2-Theta °	I. Breadth 2-Theta °
Marot									
1	MAR-2-1(1A)	0.15	0.20	4	10	35	52	0.301	0.474
2	MAR-2-2A(1)	1.65	1.70	4	7	40	49	0.294	0.462
3	MAR-2-2A(2)	2.08	2.14	5	8	36	50	0.27	0.426
4	MAR-2-2A(3)	2.64	2.69	3	7	31	60	0.278	0.411
5	MAR-2-2B(4)	3.03	3.08	6	8	33	53	0.314	0.454
6	MAR-2-2B(5)	3.74	3.79	5	7	35	53	0.293	0.456
7	MAR-2-3A(6)	4.32	4.37	5	11	39	45	0.296	0.453
8	MAR-2-3A(7)	5.07	5.12	4	7	37	51	0.29	0.437
9	MAR-2-3A(8)	5.47	5.52	5	8	36	51	0.289	0.442
10	MAR-2-3A(9)	5.65	5.70	4	6	34	56	0.27	0.416
11	MAR-2-4A(10)	6.20	6.27	3	6	35	56	0.265	0.433
12	MAR-2-4B(11)	7.20	7.25	5	6	35	54	0.286	0.441
13	MAR-2-5A(12)	8.58	8.63	3	6	30	62	0.256	0.386
14	MAR-2-5A(13)	8.78	8.83	4	6	39	50	0.259	0.425
15	MAR-2-5A(14)	8.98	9.03	3	4	30	62	0.27	0.41
16	MAR-2-5B(15)	9.57	9.62	4	6	37	53	0.278	0.443
17	MAR-2-5B(16)	9.77	9.81	3	6	28	63	0.253	0.388
18	MAR-2-6A(17)	11.58	11.61	2	6	36	56	0.238	0.386
19	MAR-2-6A(18)	11.76	11.82	3	5	30	62	0.242	0.361
20	MAR-2-6A(19)	12.00	12.05	4	6	45	44	0.269	0.432
21	MAR-2-6B(20)	12.35	12.41	3	6	43	48	0.249	0.4
22	MAR-2-6B(21)	12.51	12.54	4	7	44	46	0.291	0.453
23	MAR-2-6B(22)	13.08	13.13	4	6	37	54	0.272	0.457
24	MAR-2-6B(23)	13.34	13.38	4	5	45	46	0.267	0.448
25	MAR-2-7A(24)	14.13	14.18	2	6	34	58	0.232	0.371
26	MAR-2-7B(25)	16.03	16.08	2	5	25	68	0.242	0.374
27	MAR-2-7C(26)	16.93	16.98	2	4	32	62	0.262	0.384
28	MAR-2-9(27)	21.02	21.07	2	6	37	55	0.253	0.393
29	MAR-2-9(28)	21.22	21.26	2	10	57	32	0.281	0.468
30	MAR-2-10A(29)	24.17	24.22	2	8	49	41	0.266	0.455
31	MAR-2-10B(31)	25.90	25.95	2	7	44	48	0.279	0.493
32	MAR-2-10B(32)	26.58	26.63	3	8	58	32	0.283	0.532
33	MAR-2-11B(35)	28.91	28.96	3	9	60	27	0.274	0.484
34	MAR-2-12B(37)	30.81	30.86	2	5	28	64	0.241	0.387
35	MAR-2-12C(38)	32.24	32.30	2	6	34	58	0.254	0.399
36	MAR-2-13A(39)	32.71	32.76	2	5	30	62	0.228	0.369
37	MAR-2-13A(40)	33.73	33.78	2	6	32	60	0.258	0.409
38	MAR-2-13B(41)	34.53	34.58	2	7	36	56	0.251	0.399
39	MAR-2-13B(42)	35.51	35.56	2	6	34	58	0.253	0.397
40	MAR-2-14A(43)	35.86	35.92	3	6	38	53	0.265	0.404
41	MAR-2-14A(44)	36.76	36.81	2	6	34	58	0.253	0.401
42	MAR-2-14B(45)	37.48	37.53	3	6	35	57	0.241	0.383
43	MAR-2-14B(46)	38.38	38.44	2	6	34	59	0.264	0.409
44	MAR-2-15A(47)	39.00	39.06	2	6	29	63	0.255	0.407
45	MAR-2-15B(48)	39.86	39.92	3	5	35	57	0.251	0.403
46	MAR-2-15B(49)	41.11	41.16	2	6	35	56	0.26	0.41
Tilwalla									
1	Till-3-1A	0.30	0.33	5	8	40	46	0.299	0.451
2	Till-3-2	0.58	0.60	6	5	38	50	0.291	0.45
3	Till-3-3	0.84	0.86	4	7	40	50	0.304	0.468
4	Till-3-4	1.25	1.30	3	7	40	50	0.289	0.44
5	Till-3-5	1.53	1.58	4	7	34	55	0.308	0.451
6	Till-3-6	1.93	1.98	5	8	39	49	0.284	0.425

Table S1.

Sr. No.	Sample No.	Depth (m)		Kaolinite	Chlorite	illite	Smectite	FWHM	I. Breadth
				relative weight (%)				2-Theta °	2-Theta °
7	Till-3-7	3.15	3.18	4	7	34	55	0.302	0.457
8	Till-3-8	3.36	3.39	4	7	38	51	0.279	0.438
9	Till-3-9	3.61	3.64	4	7	37	53	0.289	0.463
10	Till-3-10	3.92	3.97	4	7	41	48	0.313	0.468
11	Till-3-11	4.49	4.54	5	7	37	51	0.301	0.478
12	Till-3-12	5.88	5.93	2	6	40	52	0.268	0.438
13	Till-3-13	6.38	6.43	4	10	58	29	0.254	0.432
14	Till-3-14	6.89	6.94	2	9	58	31	0.302	0.496
15	Till-3-15	8.73	8.78	2	5	34	59	0.259	0.401
16	Till-3-16	9.13	9.18	2	6	30	63	0.24	0.378
17	Till-3-17	9.53	9.58	1	9	59	31	0.336	0.504
18	Till-3-18	9.85	9.90	4	7	36	53	0.336	0.506
19	Till-3-19	10.05	10.10	2	7	46	46	0.316	0.516
20	Till-3-20	11.88	11.93	3	9	58	30	0.325	0.49
21	Till-3-21	12.08	12.13	2	10	59	29	0.278	0.445
22	Till-3-22	12.48	12.53	1	11	43	45	0.294	0.463
23	Till-3-23	12.88	12.93	1	8	56	34	0.304	0.477
24	Till-3-24	13.10	13.15	2	9	51	39	0.284	0.491
25	Till-3-25	13.40	13.45	2	11	59	28	0.261	0.433
26	Till-3-26	13.70	13.75	2	8	51	38	0.294	0.48
27	Till-3-27	14.95	14.99	2	11	53	34	0.281	0.453
28	Till-3-28	15.95	16.00	1	9	58	32	0.273	0.432
29	Till-3-29	16.93	16.97	1	8	51	40	0.278	0.45
30	Till-3-30	18.10	18.15	1	7	24	57	0.228	0.382
31	Till-3-31	19.58	19.63	1	8	54	36	0.289	0.458
32	Till-3-32	20.09	20.14	1	10	50	39	0.264	0.429
33	Till-3-33	20.58	20.63	1	7	43	48	0.272	0.44
34	Till-3-34	20.87	20.92	2	8	52	38	0.288	0.454
35	Till-3-35	21.90	21.95	1	8	45	46	0.26	0.421
36	Till-3-36	22.30	22.35	1	8	64	27	0.364	0.513
37	Till-3-37	22.60	22.65	1	12	56	32	0.227	0.341
38	Till-3-38	23.00	23.05	2	9	47	42	0.255	0.393
39	Till-3-39	24.37	24.42	2	6	31	60	0.239	0.359
40	Till-3-40	24.97	25.03	2	6	28	64	0.237	0.362
41	Till-3-41	27.03	27.08	2	7	28	63	0.237	0.369
42	Till-3-42	27.59	27.64	2	6	30	62	0.248	0.366
43	Till-3-43	28.22	28.27	2	5	28	65	0.231	0.362
44	Till-3-44	28.67	28.72	2	6	31	62	0.223	0.338
45	Till-3-45	29.32	29.37	2	7	44	47	0.298	0.469
46	Till-3-46	33.02	33.07	2	6	32	60	0.239	0.371
47	Till-3-47	33.52	33.57	1	7	38	54	0.242	0.39
48	Till-3-48	34.42	34.47	2	6	31	61	0.233	0.369
49	Till-3-49	34.77	34.82	1	8	43	48	0.277	0.422
50	Till-3-50	35.37	35.82	2	6	31	62	0.242	0.387
51	Till-3-51	36.36	36.41	1	8	55	36	0.321	0.475
52	Till-3-52	37.45	37.50	1	8	66	25	0.335	0.48
53	Till-3-53	39.31	39.36	3	7	44	45	0.268	0.426
54	Till-3-54	40.04	40.09	2	6	31	61	0.256	0.375
55	Till-3-55	40.64	40.69	2	8	36	54	0.23	0.34
56	Till-3-56	41.04	41.09	1	9	44	46	0.228	0.352
57	Till-3-57	41.64	41.69	2	8	43	47	0.251	0.399
58	Till-3-58	42.24	42.29	2	10	41	47	0.236	0.363
59	Till-3-59	42.77	42.82	2	7	31	60	0.249	0.396
60	Till-3-60	43.69	43.74	2	9	41	47	0.248	0.387

Table S1.

Fort Abbas

Sr. No.	Sample ID	Depth (cm)		Kaolinite	Chlorite	Illite	Smectite	FWHM	I. Breadth
				relative weight (%)				2-Theta °	2-Theta °
61	Till-3-61	44.38	44.58	2	8	35	55	0.258	0.399
62	Till-3-62	45.08	45.13	2	7	31	60	0.246	0.382
1	080421-3-1	90	100	3	6	45	46	0.338	0.546
2	080421-3-2	120	125	5	8	39	48	0.301	0.483
3	080421-3-3	140	150	3	8	36	53	0.353	0.504
4	080421-3-4	160	165	4	7	37	52	0.289	0.467
5	080421-3-5	175	180	5	8	39	48	0.279	0.447
6	080421-3-6	185	190	5	8	40	47	0.286	0.454
7	080421-3-7	195	200	5	8	39	48	0.261	0.442
8	080421-3-8	210	215	3	7	42	48	0.287	0.457
9	080421-3-9	220	225	5	8	42	46	0.271	0.456
10	080421-3-10	230	235	4	8	34	54	0.295	0.464
11	080421-3-11	240	245	5	7	41	48	0.283	0.465
12	080421-3-12	260	270	5	7	39	50	0.285	0.455
13	080421-3-13	280	290	4	7	32	57	0.303	0.478
14	080421-3-14	300	310	4	6	37	53	0.272	0.439
15	080421-3-15	320	330	5	8	38	49	0.35	0.54
16	080421-3-16	340	350	5	6	35	53	0.292	0.455
17	080421-3-17	360	370	5	6	32	57	0.266	0.424
18	080421-3-18	380	390	4	7	39	50	0.278	0.448
19	080421-3-19	395	400	3	6	40	51	0.255	0.403

Fort Derawar

1	080422-6-1	80	93	4	8	39	48	0.302	0.483
2	080422-6-2	130	140	5	11	38	46	0.293	0.472
3	080422-6-3	160	170	4	9	41	46	0.275	0.467
4	080422-6-4	195	202	5	9	46	41	0.271	0.456
5	080422-6-5	212	217	3	8	50	39	0.247	0.427
6	080422-6-6	230	240	3	9	43	45	0.25	0.441
7	080422-6-7	259	264	4	9	45	42	0.25	0.425
8	080422-6-8	286	291	3	8	40	49	0.236	0.403
9	080422-6-9	307	312	3	8	39	49	0.239	0.4
10	080422-6-10	324	329	3	9	44	45	0.23	0.391
11	080422-6-11	335	340	4	8	45	43	0.279	0.46
12	080422-6-12	348	352	2	8	42	48	0.259	0.45
14	080422-6-14	370	375	3	8	41	48	0.259	0.434
15	080422-6-16	390	400	2	7	34	57	0.241	0.409

Nara

1	NA-1-1	0.6	0.65	1	8	46	45	0.321	0.503
2	NA-1-2	3.35	3.4	3	10	42	44	0.309	0.505
3	NA-1-3	5.08	5.13	3	9	44	43	0.307	0.492
4	NA-1-4	5.88	5.93	4	9	42	45	0.291	0.464
5	NA-1-5	8.22	8.26	2	13	58	27	0.308	0.438
6	NA-1-6	11.47	11.57	2	6	33	59	0.287	0.438
7	NA-1-7	14.02	14.08	1	6	25	68	0.279	0.398
8	NA-1-8	20.17	20.22	2	7	27	64	0.283	0.466
9	NA-1-9	20.52	20.55	3	8	30	59	0.283	0.479
10	NA-1-9A	23.18	23.23	1	4	20	74	0.242	0.362
11	NA-1-10	24.08	24.13	4	8	31	57	0.284	0.474
12	NA-1-11	26.16	26.2	3	10	55	32	0.325	0.525
13	NA-1-12	26.62	26.67	1	10	57	32	0.324	0.494
14	NA-1-13	29.36	29.42	1	7	22	70	0.214	0.319

Table S2.

		Depth (m)			Kaolinite	Chlorite	Illite	Smectite	FWHM	I. Breadth
Sr. No.	Sample ID	from	to	Age (yr)	relative (%)				Δ2-Theta °	Δ2-Theta °
1	KB-3-3	6.33	6.21	77.16	1	8	41	50	0.363	0.562
2	KB-8-2	20.52	20.62	341.27	2	8	43	47	0.355	0.546
3	KB-11-1	29.62	29.72	2427.06	4	8	39	50	0.298	0.466
4	KB-13-1	35.66	35.76	4029.00	4	8	39	49	0.32	0.516
5	KB-15-3	42.85	42.95	5963.45	2	9	42	47	0.255	0.426
6	KB-17-3	49.05	49.15	7334.56	3	9	34	54	0.281	0.469
7	KB-17-2	49.55	49.65	7396.65	3	7	39	51	0.344	0.545
8	KB-19-3	55.49	55.49	8134.25	3	8	40	49	0.322	0.502
9	KB-21-1	60.38	60.52	8566.67	3	8	42	47	0.312	0.539
10	KB-22-2	62.79	62.94	8767.50	3	9	45	43	0.297	0.495
11	KB-23-4	67.67	67.71	9172.11	5	10	41	44	0.312	0.527
12	KB-25-1	72.28	72.38	9500.39	3	10	42	45	0.291	0.479
13	KB-26-3	75.18	75.25	9706.91	4	11	45	40	0.295	0.47
14	KB-27-2	77.31	77.46	9858.59	3	8	40	49	0.327	0.542
15	KB-28-3	81.25	81.35	10293.77	3	8	42	46	0.33	0.52
16	KB-29-2	83.00	83.10	10430.85	3	10	42	45	0.286	0.454
17	KB-29-1	83.40	83.50	10381.84	3	12	48	37	0.283	0.45
18	KB-30-1	85.95	86.05	10743.32	3	9	45	43	0.301	0.484
19	KB-30-2	86.25	86.35	10780.08	3	11	42	44	0.285	0.441
20	KB-31-2	87.27	87.42	10993.30	3	8	42	46	0.317	0.509
21	KB-31-1	87.99	88.14	10905.07	3	8	42	47	0.341	0.544
22	KB-32-2	90.37	91.20	11284.94	3	8	46	43	0.328	0.527
23	KB-32-3	91.32	91.47	11401.35	3	8	45	44	0.337	0.535
24	KB-34-2	96.62	96.77	12050.79	3	10	51	35	0.282	0.465
25	KB-35-1	100.22	100.37	12491.93	2	7	46	45	0.376	0.552
26	KB-36-2	102.51	102.66	12688.05	2	8	47	42	0.359	0.559
27	KB-37-2	107.41	107.56	12872.66	3	10	52	35	0.302	0.487
28	KB-38-2	108.81	108.96	12925.40	3	10	47	40	0.301	0.482
29	KB-40-2	114.91	115.06	13155.22	2	9	49	40	0.355	0.547
30	KB-41-1	119.65	120.40	20000.00	4	10	39	47	0.289	0.474